

# A Novel Loop Filter Design for Phase-Locked Loops

Y.S. Chou, W.L. Mao, Y.C. Chen and F.R. Chang

**Abstract**—A new loop filter design method for phase locked loops (PLLs) is presented, which employs multi-objective control technique to deal with the various design objectives: small noise bandwidth, good transient response (small settling time, small overshoot), and large gain and phase margins. Trade-off among the conflicting objectives is made via recently developed convex optimization skill in conjunction with appropriate adjustment of certain design parameters. One salient feature of the proposed method is that it allows one to specify the filter poles in advance, including the special case of PI form filter. Moreover, the proposed method is applicable to PLL of any order. Numerical simulation on nonlinear PLL model is performed which demonstrates the effectiveness of the proposed method.

## I. INTRODUCTION

SINCE its invention, the PLL principle [1], [2], [3], [4] has been used in a wide spread of applications, such as carrier phase tracking [5], timing recovery [6], and servo control [7], [8], etc [9]. From the system's point of view, PLL is essentially a nonlinear system. The design of PLL with a sinusoidal phase detector using Lyapunov redesign technique can be found in [10], [11]. However, there is a difficulty in applying the proposed method to high order loops. Recently, a method based on linear model approximation was proposed which designs a loop filter that minimizes the phase error variance with guaranteed gain margin and phase margin in the presence of phase detector gain uncertainty and open loop delay [12]. Coprime factorization control theory [13] and quantitative feedback theory (QFT) [14] are integrated to provide a complicated design procedure. In many cases, PI form filter which have all of the poles at the origin are favorable for some advantages [3] they brought in: infinite hold range (theoretically), infinite pull-in range (theoretically), and good phase tracking capability. However, the filters obtained by the approach just mentioned usually have poles not at the origin. Having noticed this point, an independent design procedure of PI form filter has also been addressed in [12] for second order loop. Nevertheless, it can be checked that it is hard to extend the method therein to higher order loops. In [15] the same problem is studied using another approach. Similarly, the filters obtained are generally not of PI

form.

For global positioning systems (GPS) application it is well known that the motion of the GPS satellites as well as the GPS receiver cause to Doppler effect, which in turn results in frequency shifts in the carrier and the code. Phase-locked loops are used to track the signals (carrier and C/A code). A generic PLL loop filter design for GPS receiver can be found in [16, 17], where the loop filters obtained are of PI form. In this paper, based on the commonly used voltage-controlled oscillator (VCO) model (an integrator), we propose a new loop filter design method which allows one to specify the filter poles in advance (including the special case of PI form filter). Meanwhile, the various design objectives: small noise bandwidth, good transient response [18], and large gain and phase margins [18] are all taken into consideration. Trade-off among them is made via linear matrix inequality (LMI) optimization [19], [20], [21], [22] in conjunction with appropriate adjustment of certain design parameters.

The paper is organized as follows. In Section II, the preliminaries and problem statement are given. In Section III, the new loop filter design method is presented. Section IV shows the simulation results. Comparison between the generic GPS PLL design and our method is made. Finally, Section V gives the conclusion. The detailed definitions of the  $H_2$  and  $H_\infty$  norm of stable transfer functions can be found in [22].

## II. PRELIMINARIES AND PROBLEM STATEMENT

### A. Basic model of PLL

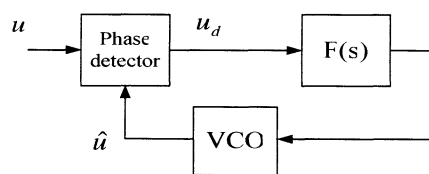


Fig.1 PLL schematic model

The PLL model used here is depicted in Fig. 1, which consists of a phase detector, low-pass loop filter  $F(s)$ , and VCO. The inputs to the phase detector are the two signals: the sum of the carrier and bandpass noise  $n(t)$  [4], i.e.,

$$u(t) = \sqrt{2}A_d \sin(\omega_0 t + w_\theta(t)) + n(t),$$

and the VCO output

$$\hat{u}(t) = \sqrt{2} \cos(\omega_0 t + \hat{w}_\theta(t)).$$

The phase detector produces, assuming the high frequency term is eliminated by the low-pass filter, the output signal

$$u_d(t) = A_d [\sin(w_\theta - \hat{w}_\theta) + w_n(t)]$$

Y.S. Chou is with the Department of Electrical Engineering, Tamkang University, Taipei county, Taiwan (phone: 02-26215656 ext 3293; fax: 02-262 09814; e-mail: yung@ee.tku.edu.tw)

M.L. Mao is with the Department of Electrical Engineering, Mingchi University of Technology, Taipei county, Taiwan (e-mail: wlmao123@yahoo.com.tw)

F.R. Chang and Y.C. Chen are with the Department of Electrical Engineering, National Taiwan University, Taipei, Taiwan. (e-mail: frchang@cc.ee.ntu.edu.tw, r93921061@ntu.edu.tw)

where  $w_n(t)$  represents the net effect caused by the noise  $n(t)$ . For small phase errors, the PLL can be further approximated by the linear model as depicted in Fig. 2.

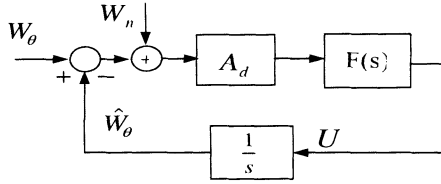


Fig. 2 PLL linear model approximation

### B. The goal

In view of Fig. 2, the goal of this paper is to design a filter  $F(s)$  to achieve the following objectives:

- (i) Closed-loop stability,
- (ii) Perfect asymptotical tracking (i.e.  $e(\infty) = 0$ ) subject to the deterministic test signals  $w_\theta(t) = t^k$ ,  $k = 0, 1, 2, \dots, m$  with  $w_n = 0$ ,
- (iii) Good transient response (i.e., small settling time, small overshoot, etc),
- (iv) Noise attenuation (assuming  $w_n$  to be white noise with zero mean),
- (v) Large stability margin (i.e. gain margin, phase margin).

Note that the variance of VCO output phase is given by

$$\sigma_{\hat{w}_\theta}^2 = \frac{1}{2\pi} \int_{-\infty}^{\infty} |T_{\hat{w}_\theta w_n}(j\omega)|^2 \Phi_{w_n}(\omega) d\omega$$

where  $T_{\hat{w}_\theta w_n}$  represents the transfer function from  $w_n$  to  $\hat{w}_\theta$ , and  $\Phi_{w_n}(\omega)$  is the power spectral density (PSD) function of the noise  $w_n$ . If  $w_n$  is white Gaussian, i.e.,  $\Phi_{w_n}(\omega) = N_0$ , then

$$\sigma_{\hat{w}_\theta}^2 = N_0 \|T_{\hat{w}_\theta w_n}(s)\|_2^2 = 2N_0 B_n$$

where  $B_n(Hz)$  denotes the noise bandwidth of  $T_{\hat{w}_\theta w_n}(s)$ . It is clear that small noise bandwidth  $B_n$  leads to small variance of the VCO output phase. In terms of the loop filter design, this can be achieved by minimizing the  $H_2$  norm of the closed-loop transfer function  $T_{\hat{w}_\theta w_n}$  over all the stabilizing filters.

On the other hand, the open-loop response should have enough gain and phase margins in order to guarantee good relative stability and well-behaved closed-loop response. It is mentioned in [12], [14] that these margins can be determined by the  $H_\infty$  norm upper bounds of certain closed-loop transfer functions. Specifically, let  $L(s)$  denote the open loop transfer function of Fig. 2. Assume a constant  $\gamma$  or alternatively a constant  $\delta$  satisfies the following  $H_\infty$  norm condition:

$$\left| \frac{L(j\omega)}{1+L(j\omega)} \right| < \gamma \quad \left( \text{resp.} \quad \left| \frac{1}{1+L(j\omega)} \right| < \delta \right) \quad (1)$$

A pair of lower bounds of the gain and phase margins is then

determined by the formulas:

$$20 \log \frac{\gamma+1}{\gamma} \text{ dB}, \quad 2 \sin^{-1} \frac{1}{2\gamma} \text{ deg} \quad \left( \text{resp.} \quad 20 \log \frac{\delta}{\delta-1} \text{ dB}, \quad 2 \sin^{-1} \frac{1}{2\delta} \text{ deg} \right) \quad (2)$$

Note that condition (1) is equivalent to a  $H_\infty$  norm bound constraint of the closed-loop transfer function  $T_{\hat{w}_\theta w_\theta}$ . Thus minimizing the  $H_\infty$  norm of the closed-loop transfer function  $T_{\hat{w}_\theta w_\theta}$  over all the stabilizing filters is expected to increase the gain and phase margins.

### C. Generic GPS PLL design

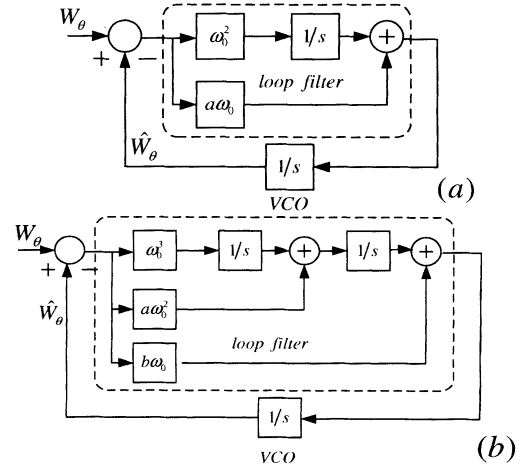


Fig. 3. (a) second order loop (b) third order loop

In the subsection, generic GPS PLL design with PI form loop filter is introduced [16, 17]. For second order PLL, see Fig. 3(a), the loop filter is assumed to be of the form

$$F(s) = a\omega_0 + \frac{\omega_0^2}{s}.$$

Hence, the closed-loop transfer function from  $w_\theta$  to  $w_\theta$  is given by the ratio of the Laplace transforms of  $w_\theta$  and  $\hat{w}_\theta$ , i.e.,

$$T_2(s) = \frac{\hat{W}_\theta}{W_\theta} = \frac{a\omega_0 s + \omega_0^2}{s^2 + a\omega_0 s + \omega_0^2}.$$

The design parameter  $a$  is usually chosen to be  $\sqrt{2}$ , which yields damping ratio  $1/\sqrt{2}$ . Furthermore, this leads to the following useful relationship:

$$\frac{B_n}{\omega_0} = \frac{1+a^2}{4a} = 0.53.$$

Similarly, for third order loop (with reference to Fig. 3(b))

$$F(s) = b\omega_0 + \frac{a\omega_0^2}{s} + \frac{\omega_0^3}{s^2},$$

$$T_3(s) = \frac{\hat{W}_\theta}{W_\theta} = \frac{b\omega_0 s^2 + a\omega_0^2 s + \omega_0^3}{s^3 + b\omega_0 s^2 + a\omega_0^2 s + \omega_0^3},$$

$$\frac{B_n}{\omega_0} = \frac{ab^2 + a^2 - b}{4(ab-1)} = 0.7845, \text{ if } a = 1.1, b = 2.4.$$

For fourth order loop

$$F(s) = c\omega_0 + \frac{b\omega_0^2}{s} + \frac{a\omega_0^3}{s^2} + \frac{\omega_0^4}{s^3},$$

$$T_4 = \frac{\hat{W}_\theta}{W_\theta} = \frac{c\omega_0 s^3 + b\omega_0^2 s^2 + a\omega_0^3 s + \omega_0^4}{s^4 + c\omega_0 s^3 + b\omega_0^2 s^2 + a\omega_0^3 s + \omega_0^4},$$

$$\frac{B_n}{\omega_0} = \frac{c^2(ab-c) + a(b^2-ac-1) - bc}{4(abc-a^2-c^2)} = 1.057,$$

if  $a = 1.35, b = 2.65, c = 2.5$ .

Note that the transfer function  $T_{\hat{w}_\theta w_\theta}$  of Fig. 3 is equal to the transfer function  $T_{\hat{w}_\theta w_\theta}$  or  $T_{\hat{w}_\theta w_n}$  of Fig. 2 when the phase detector gain  $A_d$  is assumed to be unity. On the other hand, small noise bandwidth  $B_n$  can be achieved by choosing small value of  $\omega_0$  for all the loops. However, it is evident that transients may be sacrificed with such a choice.

#### D. Useful Analysis LMIs

In the following, Lemma 1 [20] and Lemma 2 [20] present the  $H_2$  and  $H_\infty$  norm constraints of a LTI system in terms of LMIs, respectively. Lemma 3 [21] and lemma 4 [21] state that all the eigenvalues of a square matrix lie in a prescribed region if and only if certain LMIs are feasible.

**Lemma 1 [20]:** Given a LTI system  $H(s) = C(sI - A)^{-1}B + D$ , and a positive value  $\nu$ . The following statements are equivalent.

- (i)  $D = 0$  and the LTI system  $H(s)$  is stable and  $\|H(s)\|_2 < \nu$ .
- (ii)  $D = 0$  and there exist matrices  $P = P^T$  and  $Q = Q^T$  such that the following LMIs hold,

$$\begin{pmatrix} AP + PA^T & B \\ B^T & -I \end{pmatrix} < 0,$$

$$\begin{pmatrix} P & (CP)^T \\ CP & Q \end{pmatrix} > 0,$$

$$\text{Tr}(Q) < \nu^2.$$

**Lemma 2 [20]:** Given a LTI system  $H(s) = C(sI - A)^{-1}B + D$ , and a positive value  $\gamma$ . The following statements are equivalent.

- (i) The LTI system  $H(s)$  is stable and  $\|H(s)\|_\infty < \gamma$ .
- (ii) There exists a matrix  $P = P^T$  such that the following LMIs hold,

$$\begin{pmatrix} AP + PA^T & B & (CP)^T \\ B^T & -\gamma I & D^T \\ CP & D & -\gamma I \end{pmatrix} < 0,$$

$$P > 0.$$

**Lemma 3 [21]:** Given a square matrix  $A$ , all the eigenvalues of  $A$  lie in the conic sector as shown in Fig. 4(a) if and only if there exists a matrix  $X = X^T$  such that the following LMIs are satisfied,

$$\begin{pmatrix} \sin(\theta)(AX + XA^T) & \cos(\theta)(AX - XA^T) \\ \cos(\theta)(XA^T - AX) & \sin(\theta)(AX + XA^T) \end{pmatrix} < 0,$$

$$X > 0.$$

**Lemma 4 [21]:** Given a square matrix  $A$ , all the eigenvalues of  $A$  lie in the vertical strip  $(-h_1, -h_2)$  as shown in Fig. 4(b) if and only if there exists a matrix  $X = X^T$  such that the following LMIs are satisfied,

$$-2h_1 X - AX - XA^T < 0,$$

$$2h_2 X + AX + XA^T < 0,$$

$$X > 0.$$

Note that for standard second-order systems and their approximations, placing the dominant poles in the conic sector region (see Fig. 4(a)) with smaller  $\theta$  results in smaller percent overshoot [18]. Similarly, placing the dominant poles in the vertical strip (see Fig. 4(b)) with larger  $h_2$  results in smaller settling time [18].

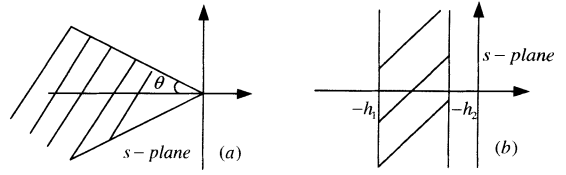


Fig.4 (a) conic sector (b) vertical strip  $(-h_1, -h_2)$

### III. FIXED-POLE LOOP FILTER DESIGN

In this section, a new method is proposed to design the loop filter for PLLs. Firstly in part A, we generalize the technique in [24] to transform the problem of designing a class of fixed-pole dynamic filter into a static state feedback synthesis problem. Secondly, in part B, multi-objective state feedback synthesis technique is employed to find a loop filter to satisfy the design objectives mentioned in section 2.

#### A. Problem reformulation

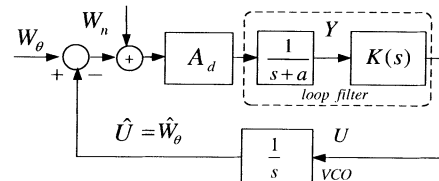


Fig.5 The reconstruction model of the PLL

Fig. 2 is redrawn as Fig. 5 with loop filter  $F(s)$  of the form

$$F(s) = \frac{1}{s+a} K(s) = \frac{s}{s+a} \left[ \sum_{l=0}^m \frac{f_l}{s^l} + \sum_{i=m+1}^{m+l} \frac{f_i}{s - \beta_{i-m}} \right] \quad (3)$$

where  $a, \beta_{j,s}$  are the poles of the filter predetermined. Let  $l=0$  denote the case that the component functions with poles at  $\beta_{i-m}$  for all  $i$  are not considered in (3), i.e.,

$$F(s) = \frac{s}{s+a} \left[ \sum_{l=0}^m \frac{f_l}{s^l} \right].$$

If the value of  $a$  is set to be zero, then  $F(s)$  is of PI form.

In view of Fig. 5, the signal  $Y(s)$  can be described by

$$Y(s) = \frac{A_d}{s+a} \left( W_n(s) + W_\theta(s) - \frac{1}{s} U(s) \right) \quad (4)$$

Define state vector  $\bar{\xi}(s)$  as follows:

$$\bar{\xi}(s) = \left[ Y(s), \frac{1}{s}Y(s), \dots, \frac{1}{s^m}Y(s), \frac{1}{s-\beta_1}Y(s), \dots, \frac{1}{s-\beta_l}Y(s) \right]^T$$

$$= [\xi_1(s), \xi_2(s), \xi_3(s), \dots, \xi_{m+l+1}(s)]^T$$

and set  $Z(s) = \hat{U}(s) = 1/s \cdot U(s)$  and  $\bar{Y}(s) = \bar{\xi}(s)$ . Then (4) becomes

$$s\xi_1(s) = -a\xi_1(s) + A_d W_n(s) + A_d W_\theta(s) - A_d \hat{U}(s)$$

Moreover,

$$\begin{cases} s\xi_i(s) = \xi_{i-1}(s) & \text{for } i = 2, 3, \dots, m+1 \\ s\xi_i(s) = \beta_{i-m-1} \cdot \xi_i(s) + \xi_1 & \text{for } i = m+2, \dots, m+l+1 \end{cases}$$

With the notation defined above it is easy to check that the dynamic filter of the prescribed form (3) is converted into a static state feedback in the new coordinate, i.e.,  $\hat{U}(s) = F_s \cdot \bar{Y}$  where  $F_s = [f_0, \dots, f_{m+l}]$ . Thus the original fixed-pole dynamic filter design problem is equivalently transformed to a static state feedback control problem as illustrated in Fig. 6 with  $G$  described by

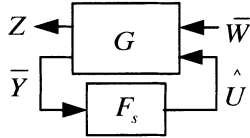


Fig.6 The equivalent state feedback model

$$G \begin{cases} s\bar{\xi}(s) = A\bar{\xi}(s) + B_1\bar{W}(s) + B_2\hat{U}(s) \\ Z(s) = D_{12}\hat{U}(s) \\ \bar{Y}(s) = \bar{\xi}(s) \end{cases}$$

where  $\bar{W} = [W_n \quad W_\theta]^T$ ,

$$A = \begin{bmatrix} -a & 0 & \dots & 0 & 0 & 0 & \dots & \dots & 0 \\ 1 & 0 & \dots & 0 & 0 & 0 & 0 & \dots & 0 \\ 0 & 1 & \ddots & \vdots & \vdots & 0 & \ddots & \ddots & \vdots \\ \vdots & \ddots & \ddots & 0 & 0 & \vdots & \ddots & \ddots & 0 \\ 0 & \dots & 0 & 1 & 0 & 0 & \dots & 0 & 0 \\ 1 & 0 & \dots & 0 & 0 & \beta_1 & 0 & \dots & 0 \\ 1 & 0 & \ddots & \vdots & \vdots & 0 & \beta_2 & \ddots & \vdots \\ \vdots & \vdots & \ddots & 0 & 0 & \vdots & \ddots & \ddots & 0 \\ 1 & 0 & \dots & 0 & 0 & 0 & \dots & 0 & \beta_l \end{bmatrix}_{(m+l+1) \times (m+l+1)}$$

$$B_1 = \begin{bmatrix} A_d & 0 & \dots & 0 \\ A_d & 0 & \dots & 0 \end{bmatrix}_{2 \times (m+l+1)}^T,$$

$$B_2 = [-A_d \quad 0 \quad \dots \quad 0]_{1 \times (m+l+1)}^T, \quad D_{12} = 1.$$

The resulting closed-loop system from  $\bar{w}$  to  $z$  is as follows.

$$T_{z\bar{w}} \begin{cases} s\bar{\xi}(s) = (A + B_2 F_s)\bar{\xi}(s) + B_1\bar{W}(s) \\ Z(s) = F_s \bar{\xi}(s) \end{cases}$$

For  $H_2$  minimization from  $w_n$  to  $z$  (i.e., the noise bandwidth minimization problem), the closed-loop system matrix is given by

$$\begin{bmatrix} A + B_2 F_s & B_1 R_1 \\ F_s & 0 \end{bmatrix}$$

where  $R_1 = [1 \quad 0]^T$ .

For  $H_\infty$  minimization from  $w_\theta$  to  $z$  (i.e., the gain/phase margin maximization problem), the closed-loop system matrix is given by

$$\begin{bmatrix} A + B_2 F_s & B_1 R_2 \\ F_s & 0 \end{bmatrix}$$

where  $R_2 = [0 \quad 1]^T$ .

### B. LMI design of the loop filter

In order to meet the multiple design objectives mentioned in section 2, the following multi-objective control problem is considered, where  $\alpha_2$  and  $\alpha_\infty$  are weights for the trade-off of the two design objectives: noise bandwidth and gain/phase margins.

$$\text{Minimize } \alpha_2 \cdot v^2 + \alpha_\infty \cdot \gamma \quad (5)$$

over  $N \in R^{l \times (m+l+1)}$ ,  $M = M^T \in R^{(m+l+1) \times (m+l+1)}$ , and  $Q \in R$

satisfying:

$$\begin{cases} \begin{pmatrix} He(AM + B_2 N) & B_1 R_1 \\ (B_1 R_1)^T & -I \end{pmatrix} < 0 \\ \begin{pmatrix} M & N^T \\ N & Q \end{pmatrix} > 0 \\ Trace(Q) < v^2 \end{cases} \quad (6)$$

$$\begin{cases} \begin{pmatrix} He(AM + B_2 N) & B_1 R_2 & N^T \\ (B_1 R_2)^T & -\gamma I & 0 \\ N & 0 & -\gamma I \end{pmatrix} < 0 \\ M > 0 \end{cases} \quad (7)$$

$$\begin{cases} \begin{pmatrix} \sin(\theta) \cdot He(AM + B_2 N) & \cos(\theta) \cdot SH(AM + B_2 N) \\ \{\cos(\theta) \cdot SH(AM + B_2 N)\}^T & \sin(\theta) \cdot He(AM + B_2 N) \end{pmatrix} < 0 \\ M > 0 \end{cases} \quad (8)$$

$$\begin{cases} -2h_1 M - He(AM + B_2 N) < 0 \\ 2h_2 M + He(AM + B_2 N) < 0 \\ M > 0 \end{cases} \quad (9)$$

where the notation  $He(A) = A + A^T$ ,  $SH(A) = A - A^T$  are used.

Denote the optimal solution by  $(N^*, M^*, Q^*, v^*, \gamma^*)$ .

**Theorem 1:** Given the nonnegative integers  $l, m$ , the values  $a, \beta_1, \beta_2, \dots, \beta_l$ , the weights  $\alpha_2, \alpha_\infty$ , the positive values  $\theta$ , and  $h_1, h_2$  with  $h_2 < h_1$ . If the optimization problem (5) is solvable, there exists a fixed-pole loop filter  $F(s)$  of the form

$$F(s) = \frac{s}{s+a} \left[ \sum_{i=0}^m \frac{f_i}{s^i} + \sum_{i=m+1}^{m+l} \frac{f_i}{s - \beta_{i-m}} \right]$$

with  $F_s = [f_0, \dots, f_{m+l}] = N^* M^{*-1}$ , such that

(i) the closed-loop system is stable,

(ii)  $\|T_{\bar{w}_\theta \bar{w}_n}(s)\|_2 < v^*$  and  $\|T_{\bar{w}_\theta \bar{w}_\theta}(s)\|_\infty < \gamma^*$ ,

(iii) the closed-loop poles lie within the intersection of the strip  $(-h_1, -h_2)$  and the conic sector with parameter  $\theta$ .

Proof: The results follow from applying standard technique in [18]. ■

**Corollary 1:** Suppose  $a=0$ ,  $l=0$ , and  $m>0$ . There exists a  $m^{th}$ -order loop filter  $F(s)$  of the form

$$F(s) = \sum_{i=0}^m \frac{f_i}{s^i}$$

such that the resulting closed-loop system possesses the properties (i), (ii), (iii) of Theorem 1.

Three cases are discussed further for corollary 1.

**Case 1:**  $\alpha_2 = 1$ ,  $\alpha_\infty = 0$

In this case only the factors: noise bandwidth and transient response are considered for the loop filter design. This is done via performing the following  $H_2$  norm minimization subject to regional pole placement constraints:

$$\min_{\text{subject to (6),(8),(9)}} \nu^2 \quad (\text{OPT1})$$

An algorithm based on carrying out the optimization problem (OPT1) in conjunction with appropriate adjustment of the parameters  $\theta$  and  $h_2$  is presented as follows.

Algorithm 1: Given the desired noise bandwidth  $B_n^*$  (Hz) and the desired order  $m$  of the loop filter.

Step 1 Select damping ratio  $\zeta$ , e.g.  $\zeta \geq 0.707$ , i.e.  $\theta \leq \pi/4$ .

Step 2 Select  $h_2$  with reference to TABLE 1. Perform (OPT1).

Step 3 If  $B_n > B_n^*$ , decreases  $h_2$ ; otherwise, increases  $h_2$ .

Perform (OPT1) to get new value of  $B_n$ . Continue this process until  $B_n = B_n^*$ .

Step 4 If the transient response is satisfactory, the filter design is complete; otherwise continue the following steps:

Step 4.1 If it is not good enough for overshoot, we decrease  $\theta$  and perform (OPT1) to get  $B_n$ .

Go to Step 3.

Step 4.2 If it is not good enough for settling time, we increase  $\theta$  and perform (OPT1) to get  $B_n$ .

Go to Step 3.

Note that for practical situation, the noise bandwidth of the PLL of a GPS receiver is around the range 5~15 Hz [25], hence TABLE 1 is useful in selecting the parameter  $h_2$  for practical case. As for the parameter  $h_1$ , little effect has been

found on the noise bandwidth when it is far away from  $h_2$ . Moreover, it is observed that it causes to smaller noise bandwidth and larger  $\|T_{\tilde{w}_\theta \tilde{w}_\theta}(s)\|_\infty$  when it is close to  $h_2$ . Thus

the pole constraint relevant to parameter  $h_1$  is omitted in case 1. On the other hand, it is found that decreasing  $\theta$  improves overshoot; however, the noise bandwidth increases. In order to maintain the same noise bandwidth, the parameter  $h_2$  is decreased. But this leads to a larger settling time. Thus there is a trade-off between noise bandwidth and settling time. Similarly, there is a trade-off between noise bandwidth and overshoot.

**Case 2:**  $\alpha_2 = 0$ ,  $\alpha_\infty = 1$

In this case the following optimization problem is performed for the loop filter design to maximize the gain/phase margins and ensure good transient response.

$$\min_{\text{subject to (7),(8),(9)}} \gamma \quad (\text{OPT2})$$

The following relationships between the  $H_\infty$  norm and the parameters  $h_1$ ,  $h_2$  and  $\theta$  are explored: the  $H_\infty$  norm is directly proportional to  $h_2$ ,  $\theta$  and is inversely proportional to  $h_1$ . But the noise bandwidth is directly proportional to  $h_1$  in this case. Moreover, it was observed that performing (OPT2) without the LMI constraint concerning  $h_1$  usually causes some closed-loop poles to be far away from the imaginary axis. This in turn leads to large noise bandwidth. Thus the pole constraint relevant to parameter  $h_1$  is included in this case for the adjustment of the noise bandwidth.

**Case 3:**  $\alpha_2$  and  $\alpha_\infty$  are positive numbers

This case is a mixture of the former two cases. Noise bandwidth, gain/phase margins, and transient response are all taken into consideration. Without loss of generality,  $\alpha_2$  may be assumed to be unity. The loop filter design is done via performing the following optimization problem in conjunction with appropriate adjustment of the parameters  $\theta$  and  $h_1, h_2$ :

$$\min_{\text{subject to (6),(7),(8),(9)}} \nu^2 + \alpha_\infty \cdot \gamma \quad (\text{OPT3})$$

Large value for weight  $\alpha_\infty$  (i.e.,  $\alpha_\infty > 1$ ) is chosen if the gain /phase margins are emphasized. On the contrary, noise attenuation is emphasized by selecting a small weight for  $\alpha_\infty$  (i.e.,  $\alpha_\infty < 1$ ). The parameters,  $h_1$ ,  $h_2$  and  $\theta$ , are tuned with reference to Case 1 and Case 2.

**Remark 1** In the generic GPS PLL design, there is a closed form formula for the ratio  $B_n/\omega_0$  in terms of the design parameters, for example, the parameters  $a$ ,  $b$  and  $c$  for the fourth order loop (see Section 2.C). After determining the parameters through minimizing the ratio  $B_n/\omega_0$ , the ratio keeps constant. As a result, the noise bandwidth is proportional to the value of  $\omega_0$ . Smaller noise bandwidth requirement leads to smaller value of  $\omega_0$ , which causes some of the closed-loop

TABLE 1

SECOND ORDER LOOP ( $\theta = \pi/4$ )

	$h_2=7$	$h_2=10$	$h_2=13$	$h_2=16$	$h_2=19$
$B_n$ (Hz)	5.34	7.62	9.91	12.18	14.46

THIRD ORDER LOOP ( $\theta = \pi/4$ )

	$h_2=3$	$h_2=5$	$h_2=7$	$h_2=9$	$h_2=10$
$B_n$ (Hz)	4.98	8.30	11.58	14.94	16.59

FOURTH ORDER LOOP ( $\theta = \pi/4$ )

	$h_2=2$	$h_2=3$	$h_2=4$	$h_2=5$	$h_2=6$
$B_n$ (Hz)	5.37	8.07	10.74	13.47	16.16

poles to move toward the imaginary axis since the characteristic polynomial for the fourth order loop is given by  $s^4 + ca_0s^3 + ba_0^2s^2 + aa_0^3s + a_0^4$ , hence slows down the system response. Clearly, it is hard to meet the multiple objectives as mentioned in Section 2 by the single parameter  $\omega_0$ . In comparison, our method provides a flexible and general way to yield a filter via trading off the objectives through optimization over all the design parameters  $f_{i/s}$ .

#### IV. SIMULATION RESULTS

In the practical situation, the desired noise bandwidth of PLL of GPS receiver is selected to be around 15 Hz, i.e.  $B_n^* \approx 15\text{Hz}$ . Thus this design objective is enforced for all the cases discussed here. By the generic GPS PLL design described in Section 2.C, PI form filters of different orders (i.e.,  $m = 1, 2, 3$ ) are obtained once the target noise bandwidth  $B_n^*$  is given. To apply our method (corollary 1), without loss of generality, the phase detector gain  $A_d$  is assumed to be unity. TABLE 2 shows the transfer functions of the loop filters obtained by the generic GPS PLL design and our LMI approach, respectively.

TABLE 2 (A) GENERIC GPS PLL DESIGN

Loop order	Design parameters	Loop filter $F(s)$
2	$a = \sqrt{2}$ $\omega_0 = 28.30$	$40.02 + \frac{801}{s}$
3	$a = 1.1, b = 2.4$ $\omega_0 = 19.12$	$45.89 + \frac{402.2}{s} + \frac{6990}{s^2}$
4	$a = 1.35, b = 2.65, c = 2.5$ $\omega_0 = 14.19$	$35.48 + \frac{533.7}{s} + \frac{3858}{s^2} + \frac{40560}{s^3}$

TABLE 2 (B) LMI APPROACH

Loop order	Design parameters	Loop filter $F(s)$
2	$\alpha_2 = 1, \alpha_\infty = 0$ $\theta = \pi/4, h_2 = 19.7$	$40.56 + \frac{787.58}{s}$
3	$\alpha_2 = 1, \alpha_\infty = 35$ $\theta = \pi/6, h_1 = 46, h_2 = 6.4$	$47.7 + \frac{535.8}{s} + \frac{1909}{s^2}$
4	$\alpha_2 = 1, \alpha_\infty = 30$ $\theta = \pi/6, h_1 = 40, h_2 = 3.62$	$48.01 + \frac{519.5}{s} + \frac{2193}{s^2} + \frac{3358}{s^3}$

Several performance indices are evaluated for the resulting PLLs as shown in TABLE 3. For second order loop, the generic design is a near optimal design [3]. It is observed that our approach obtains a filter which results in similar performance. Moreover, for higher order loops, by our approach, there are significant improvements on the transient performance as well as the gain/phase margins over the generic design. Note that the resulting PLLs are conditionally stable systems as defined in [14], which have negative gain margins. The gain and phase margins on the list are the guaranteed values computed by the formulas (2), which imply that each of the closed loop systems remains stable if the open loop gain is decreased less than the guaranteed values.

Next we use the popular software **SystemView** Version 5.0 to simulate the resulting PLLs. A nonlinear system model, as shown in Fig. 7, is used, where the function of the phase

TABLE 3  
The performance indices for noise bandwidth 15 Hz

Design method	Loop order	Rise time (sec)	Overshoot (%)	Settling time (sec)	$H_\infty$ norm
LMI approach	2	0.03	20.3	0.175	1.26
	3	0.03	15.7	0.25	1.196
	4	0.031	15.9	0.267	1.2
Generic GPS	2	0.03	20.8	0.173	1.27
	3	0.032	23.7	0.901	1.712
	4	0.034	30.9	5.12	3.366

Design method	Loop order	Gain margin	Phase margin
LMI approach	2	5.07 dB	46.76 deg
	3	5.28 dB	49.42 deg
	4	5.26 dB	49.25 deg
Generic GPS	2	5.04 dB	46.37 deg
	3	4 dB	34 deg
	4	2.26 dB	17.09 deg

detector is modeled as  $A_d \sin(\bullet)$  instead of a constant gain  $A_d$ .

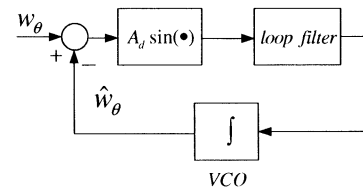


Fig. 7 The simulation model using SystemView

Third order and fourth order PLL loops are simulated for testing the lock-in performance. Theoretically, the lock range,  $\Delta\omega_l$ , is defined as the frequency range within which the PLL locks within one single beat note between the reference frequency and VCO output frequency [3]. It can be estimated by solving the following equation for  $\Delta\omega_l$  [3],

$$\Delta\omega_l = A_d |F(j\Delta\omega_l)|.$$

For third order loops, the estimated lock ranges  $\Delta\omega_l$  are 48.18 (rad/s) and 43.16 (rad/s) for LMI approach and generic design, respectively. Frequency changes within and over both of the lock ranges, equivalently a phase ramp input, are applied to the loops. The responses are shown in Fig. 8 (a) and (b). It is observed that the PLLs designed by both approaches get locked. But the transient response by LMI design looks better than that by the generic design.

Finally, same test is applied to the fourth order loops. The result is shown in Fig. 9 (a) and (b). Again the PLL design by LMI approach behaves better than that by generic design. Particularly, for higher frequency change, while the PLL by generic design loses locked, that by LMI approach still works very well as can be seen in Fig. 9(b).

#### V. CONCLUSION

We have presented a new filter design method for PLL, taking into consideration the various design objectives such as small noise bandwidth, good transient response (small settling time, small overshoot), and large gain and phase margins. In comparison with several existing methods, the proposed

method is simple and applicable to PLL of any order. Particularly, it allows one to specify the filter poles to desired locations in advance (including the special case of PI form filters which have all the poles at the origin). Numerical simulation of a GPS application was performed using nonlinear PLL model. It was observed that our method yields much better performance, when compared with the traditional GPS PLL design.

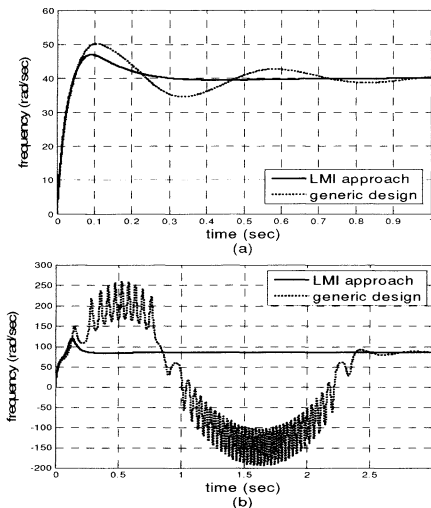


Fig. 8 The frequency of VCO output of third order loop for phase ramp input (a) 40 and (b) 85 (rad/s)

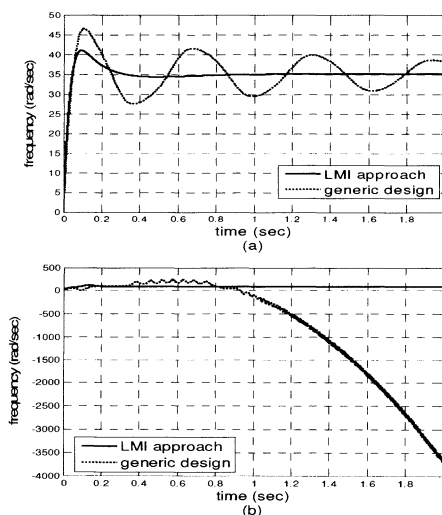


Fig.9 The frequency of VCO output of fourth order loop for phase ramp input (a) 35 and (b) 85 (rad/s)

#### ACKNOWLEDGMENT

This work was supported in part by National Science Council under Grant NSC 94-2213-E-002-079, Grant NSC 94-2213-E-032-019, and Grant NSC 90-2213-E-032-008.

#### REFERENCES

- [1] A. Blanchard, *Phase-Locked Loops: Application to Coherent Receiver Design*. Wiley: New York, 1978.
- [2] A. J. Viterbi, *Principles of Coherent Communications*. McGraw-Hill: New York, 1966.
- [3] R. E. Best, *Phase-locked loop: Design, Simulation, and Applications*, McGraw-Hill International, 1997.
- [4] F. M. Gardner, *Phaselock Techniques*. John Wiley, New York, NY, third ed., 2005.
- [5] A. Abu-Rgheff, M.N. Sumartana, I.G.G, "Carrier phase tracking in digital radio communications," *Electronics Letters*, vol. 34, pp. 2306–2307, 1998
- [6] A. De Gloria, D. Grosso, M. Olivieri, and G. Restani, "A novel stability analysis of a PLL for timing recovery in hard disk drives," *IEEE Trans. Circuits and Systems-I: Fundamental Theory and Applications*, vol. 46, no. 8, pp. 1026-1031, 1999.
- [7] M. F. Lai, M. Nakano, and G.C. Hsieh, "Application of Fuzzy logic in the phase-locked loop speed control of induction motor drive," *IEEE Trans. on Industrial Electronics*, vol. 43, no.6, pp. 630-639, 1996.
- [8] J. W. Ahn, S. G. Oh, S. Y. Pyo, C.U. Kim, and Y. M. Hwang, "Digital PLL technique for precise speed control of SR Drive, *Power Electronics Specialists Conference (PESC99) 30th Annual IEEE*, vol. 2, 1999, pp. 815 – 819.
- [9] G. C. Hsieh and J. C. Huang, Phase-Locked Loop Techniques- A Survey," *IEEE Trans on Industrial Electronics*, vol. 43, no.6, pp. 609-615, 1996.
- [10] D. Y. Abramovitch, "Analysis and design of a third order phase-lock loop," in *Proceeding of the IEEE Military Communications Conference*, vol. 2, October 1988, pp. 455-459.
- [11] D. Y. Abramovitch, "Lyapunov Redesign of analog phase-lock loops," *IEEE Trans. on Communication*, vol. 38, pp. 2197-2202, December 1990.
- [12] O. Yaniv, D. Raphaeli, "Near-optimal PLL design for decision feedback carrier and timing recovery," *IEEE Trans. on Communication*, Vol. 49, pp. 1669 - 1678, Sept. 2001.
- [13] M. Vidyasagar, *Control System Synthesis-A Factorization Approach*. MIT press, 1985.
- [14] O. Yaniv, *Quantitative Feedback Design of Linear and Nonlinear Control Systems*. Norwell, MA: Kluwer, 1999.
- [15] V. Suplin and U. Shaked, "Robust H-infinity control of phase-locked loops with polytopic type uncertainties," *Int. J. Robust and Nonlinear Control*, vol. 11, pp. 305-314, 2001.
- [16] E.D. Kaplan, *Understanding GPS: principles and application*. Artech House, London, 1996.
- [17] W. L. Mao, H. W. Tsao, and, F. R. Chang, "Intelligent GPS receiver for robust carrier phase tracking in kinematic environments," *IEE Proceedings Radar, Sonar and Navigation*, vol. 151, No. 3, pp.171-180, Jun. 2004.
- [18] N. S. Nise, *Control Systems Engineering*. John Wiley & Sons, Inc., 4<sup>th</sup> edition, 2004.
- [19] S. Boyd, L. EL Ghaoui, E. Feron, and V. Balakrishnan, *Linear Matrix Inequalities in System and Control Theory*, SIAM, Philadelphia, 1994
- [20] C. Scherer, P. Gahinet, and M. Chilali, "Multiobjective output feedback control via LMI optimization" *IEEE Trans. Autom. Control*, vol. 42, pp. 896-911, 1997
- [21] M. Chilali and P. Gahinet, "H $\infty$  design with pole placement constraints: an LMI approach," *IEEE Trans. Autom. Control*, vol. 41, pp. 358-367, 1996.
- [22] P. Gahinet, A. Nemirovski, A. Laub, and M. Chilali, *LMI Control Toolbox*, The MathWorks Inc., Natick, MA, 1995.
- [23] K. Zhou, and J. C. Doyle, *Essentials of Robust Control*, Prentice-Hall, Inc., New Jersey, 1998.
- [24] C. E. de Souza and U. Shaked, "An LMI method for output-feedback  $H_\infty$  control design for system with parameter uncertainty", in *Proc. IEEE Conf. Decision and Control*, Tampa, Florida USA, pp.1777-1779, 1998.
- [25] M. S. Braasch and A. J. Van Dierendonck, "GPS receiver architectures and measurements," in *Proceedings of the IEEE*, vol. 87, pp. 48–64, 1999.